

## Catalyst Design

International Edition: DOI: 10.1002/anie.201707670  
German Edition: DOI: 10.1002/ange.201707670

## Rational Optimization of Supramolecular Catalysts for the Rhodium-Catalyzed Asymmetric Hydrogenation Reaction

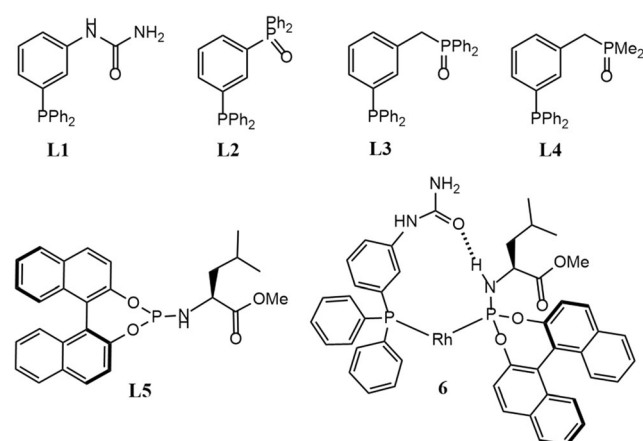
Julien Daubignard, Remko J. Detz, Anne C. H. Jans, Bas de Bruin, and Joost N. H. Reek\*

**Abstract:** Rational design of catalysts for asymmetric transformations is a longstanding challenge in the field of catalysis. In the current contribution we report a catalyst in which a hydrogen bond between the substrate and the catalyst plays a crucial role in determining the selectivity and the rate of the catalytic hydrogenation reaction, as is evident from a combination of experiments and DFT calculations. Detailed insight allowed in silico mutation of the catalyst such that only this hydrogen bond interaction is stronger, predicting that the new catalyst is faster. Indeed, we experimentally confirmed that optimization of the catalyst can be realized by increasing the hydrogen bond strength of this interaction by going from a urea to phosphine oxide H-bond acceptor on the ligand.

The asymmetric hydrogenation reaction is undoubtedly the most powerful asymmetric transformation for the fine chemical industry as it provides a rather general strategy to create chiral centers in organic molecules.<sup>[1]</sup> As the synthesis of the desired products cannot always be reached using the existing catalysts, the search for new methods and concepts has received considerable attention.<sup>[2]</sup> Combinatorial chemistry approaches and high-throughput catalyst screenings have been demonstrated to be increasingly important.<sup>[3]</sup> For the generation of catalyst libraries based on chiral ligands, the use of supramolecular ligand building blocks that form bidentate ligands by self-assembly is a powerful strategy as the number of catalysts grows exponentially with the number of synthesized building blocks.<sup>[4]</sup> Next to interactions between the two ligand building blocks, hydrogen bonding between functional groups of the substrate and the ligands at the metal complex can contribute to catalyst selectivity.<sup>[5]</sup> One of the major goals in the area of asymmetric hydrogenation, or more general in the field of catalysis, would be the rational design of transition metal catalysts. Although for several catalyst systems detailed knowledge on the reaction mechanism has been obtained,<sup>[6]</sup> prediction of the catalyst properties is still very challenging.<sup>[7]</sup>

However, when the selectivity of a catalytic reaction is controlled by supramolecular interactions, further rational optimization could be performed, guided by theoretical prediction. Herein we report the first example of rational design of a catalyst for the asymmetric hydrogenation reaction by optimization of the supramolecular interactions between the substrate and the catalyst, leading to enhanced activity and superior selectivity in the hydrogenation of hydroxy-functionalized di- and trisubstituted alkenes. In order to allow a rational approach, the reaction mechanism of the supramolecular catalyst used was investigated by means of X-ray crystallography, NMR spectroscopy, kinetic studies, and DFT calculations of the reaction pathway. Subsequently, the relevant supramolecular interactions between the substrate and the catalyst were optimized in silico, resulting in the rational design of a second generation of catalysts. Catalytic and kinetic experiments with the newly prepared catalysts confirmed that both the activity and the selectivity are improved.

We previously reported the use of complex  $[\text{Rh}(\text{L1})(\text{L5})\text{(cod)}]\text{BF}_4$  as a new selective catalyst based on a self-assembled supramolecular hetero-bidentate ligand, formed by a single hydrogen bond between the NH group of a phosphoramidite and the urea carbonyl of a urea-functionalized phosphine (Scheme 1).<sup>[8]</sup> This complex affords the highest enantioselectivity (> 99% *ee*) reported up to now for the hydrogenation of methyl 2-hydroxymethacrylate (and several of its derivatives), which upon hydrogenation forms the so-called “Roche ester”, an important intermediate in the preparation of several biologically active compounds. Catal-



**Scheme 1.** The chemical structures of the ligand building blocks with H-bond acceptors (L1–L4) and H-bond donor (L5), and a typical example of a self-assembled bidentate ligands around a rhodium complex (6).

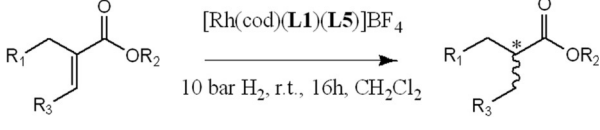
[\*] Dr. J. Daubignard, Dr. R. J. Detz, A. C. H. Jans, Prof. Dr. B. de Bruin, Prof. Dr. J. N. H. Reek

Homogeneous, Bioinspired and Supramolecular Catalysis  
van 't Hoff Institute for Molecular Sciences University of Amsterdam  
Science Park 904, 1098 XH Amsterdam (The Netherlands)  
E-mail: j.n.h.reek@uva.nl

Supporting information and the ORCID identification number(s) for the author(s) of this article can be found under <https://doi.org/10.1002/anie.201707670>.

© 2017 The Authors. Published by Wiley-VCH Verlag GmbH & Co. KGaA. This is an open access article under the terms of the Creative Commons Attribution-NonCommercial License, which permits use, distribution and reproduction in any medium, provided the original work is properly cited and is not used for commercial purposes.

**Table 1:** Asymmetric hydrogenation of methyl-2-hydroxymethylacrylate derivatives **S1–S4** catalyzed by supramolecular  $[\text{Rh}(\text{cod})(\text{L1})(\text{L5})]\text{BF}_4$ .<sup>[a]</sup>



| Substrate                | R <sub>1</sub> | R <sub>2</sub> | R <sub>3</sub>    | Conv [%] | ee [%]                |
|--------------------------|----------------|----------------|-------------------|----------|-----------------------|
| <b>S1</b> <sup>[b]</sup> | OH             | Me             | H                 | 100      | 99                    |
| <b>S2</b> <sup>[b]</sup> | OH             | tBu            | H                 | 100      | 99                    |
| <b>S3</b> <sup>[b]</sup> | OH             | Me             | Ph <sup>[d]</sup> | 83       | 96 <sup>[d]</sup> (S) |
| <b>S4</b>                | OMe            | Me             | Ph <sup>[d]</sup> | 67       | 25 (S)                |

[a]  $[\text{Rh}(\text{I})(\text{5})(\text{cod})_2] = 0.2 \text{ mM}$ ,  $[\text{substrate}] = 0.1 \text{ M}$ , solvent:  $\text{CH}_2\text{Cl}_2$ , reaction performed at 10 bar  $\text{H}_2$  pressure at 25 °C for 16 h. [b] Results previously reported in Ref. [8]. [c] ee obtained for this substrate varies between 96 and 99%. [d] E isomer.

ysis results show that hydrogen bonding between the catalyst and the substrate plays an important role for achieving this high selectivity (Table 1).

In the context of further rational optimization by computational strategies we decided to study the origin of the high selectivity in detail. The X-ray analysis of  $[\text{Rh}(\text{L1})(\text{L5})-(\text{cod})]\text{BF}_4$  as the precatalyst as well as the solvento complex that is formed after hydrogenation of the cod (1,5-cyclooctadiene), confirmed the presence of the hydrogen bond between the PNH group of the phosphoramidite and the carbonyl group of the urea-functionalized phosphine, as predicted by the DFT computed structures. (These structures will be published in a full paper.) The acetonitrile complex that was obtained after hydrogenation of the cod was also characterized in solution and in the solid state. This complex appeared to be sufficiently stable to allow further substrate coordination studies.

Upon addition of the trisubstituted alkene **S3** to a solution of the solvento complex in dichloromethane (see the Supporting Information), the substrate–catalyst complex **A** in which both the carbonyl and the alkene of the prochiral substrate are coordinated to the rhodium center was identified by NMR spectroscopy as the major species. Additional 2D  $^1\text{H}$ - $^1\text{H}$  COSY experiments and DFT calculations revealed that the hydrogen bond between the substrate and the functional group is not with the ester group of **L5**, as previously proposed.<sup>[8]</sup> Instead, the OH group inserts in the existing hydrogen bond between **L1** and **L5**, leading to the formation of two hydrogen bonds between the substrate and the complex (Figure 1). This complex was found to be  $5.45 \text{ kcal mol}^{-1}$  more stable than the alternative complexes that were computed, and as such is the major catalyst–substrate species observed in solution. The binding of substrate **S3** and **S4**, which is the methoxy protected analogue of **S3** that cannot form hydrogen bonds, to the solvento complex was also studied by UV-vis titrations. The binding of **S3** was found to be  $2 \text{ kcal mol}^{-1}$  stronger than for **S4** in line with the proposed hydrogen bond formation.

In order to further unravel the mechanism of the hydrogenation reaction with this complex as catalyst, in situ  $^{31}\text{P}$  NMR experiments were performed, indicating that the solvento complex was the resting state of the reaction. As no

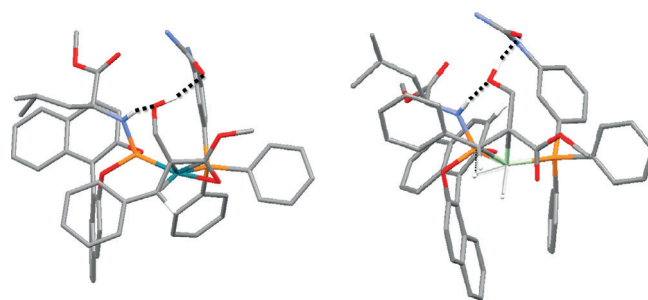
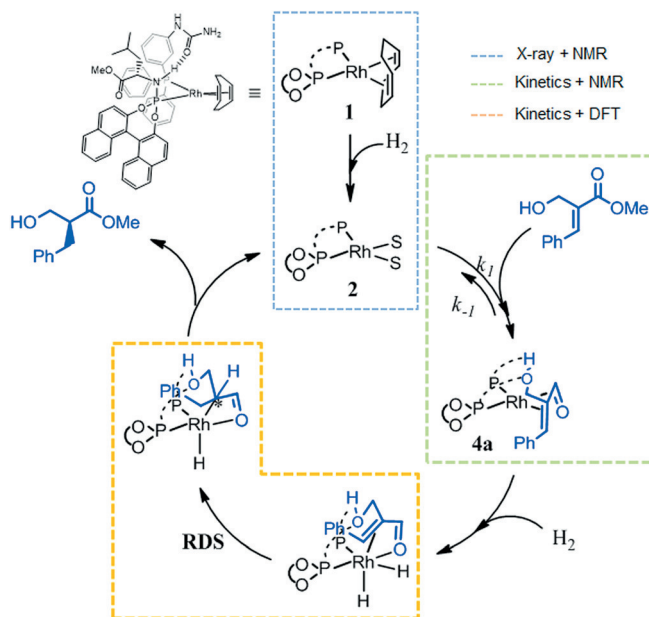


**Figure 1.** Optimized structure of the catalyst–substrate complex  $\text{Rh}(\text{L1})(\text{L5})(\text{S3})$  (left) and the rate-determining transition state of the hydride migration step (right) in which two hydrogen bonds are formed between the catalyst and **S3**.



**Scheme 2.** Proposed catalytic cycle for the supramolecular rhodium-catalyzed asymmetric hydrogenation reaction of hydroxy-functionalized alkenes.

hydrides could be detected when the complex was pressurized, the reaction follows the unsaturated pathway (as displayed in Scheme 2), meaning substrate coordination is required prior to oxidative addition of molecular hydrogen.<sup>[9]</sup> Next, a series of kinetic experiments were performed, monitored by gas uptake, to elucidate the kinetics of the reaction, which confirmed the earlier described reaction mechanism. The kinetic data obtained for both substrates **S3** and **S4** could be fitted using the Michaelis–Menten rate equation. The Michaelis–Menten constants obtained for these substrates again confirmed a stronger binding of **S3** to the rhodium complex compared to **S4**. Interestingly, also  $V_{\text{max}}$  (the maximum rate of the catalyst at substrate saturation) appeared to be higher for **S3**, suggesting that the hydrogen bond also resulted in an overall lower energy barrier. This was further studied by computing the reaction pathways using DFT calculations. A detailed computational study of the different reaction pathways (unsaturated pathway, dihydride

pathway and semi-dihydride pathway) revealed that the unsaturated pathway is energetically favored. Importantly, for the lowest energy pathway, the hydrogen bonds between the substrate and the ligands are present throughout the reaction. The rate-determining transition state is represented by the hydride migration step **B** (Scheme 2 and Figure 3), in line with the kinetic studies. Importantly, this TS structure is stabilized by the hydrogen bond to a larger extent than the substrate complex, explaining the higher  $V_{\max}$  obtained for the substrate that can form hydrogen bonds. Inspection of the structures in detail shows that the geometry of transition state is more suited to accommodate the hydrogen bonds as is reflected in the shorter NH–O and OH–carbonyl distances (Figure 1).

From this mechanistic study it is clear that hydrogen bonds between the substrate and the ligands play a crucial role in determining both the selectivity and the activity. With this knowledge in mind, we wondered if it would be possible to generate a better catalyst based on rational design by targeting these interactions. As phosphine-oxides are known to be the strongest hydrogen bond acceptors, we aimed for replacing urea-phosphine building block **L1** in the complex for a phosphine-oxide analogue. DFT-optimized structures of catalyst-substrate complexes based on building block **L2** and **L3** showed that ligand **L3** forms complexes that are structurally most similar to the parent complex (see Figure 2). Clearly,

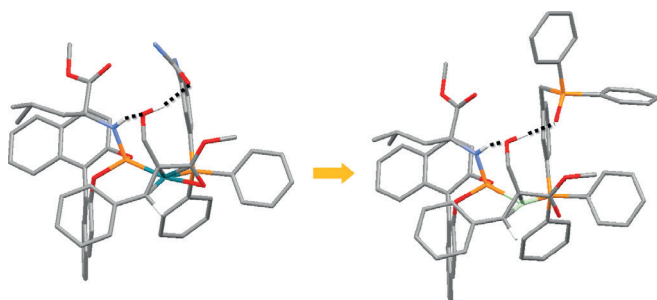


**Figure 2.** Rational optimization of supramolecular interactions in a transition metal catalyst. The crucial hydrogen bond acceptor (urea of **L1**) in the catalyst-substrate complex **A** (left structure) is replaced by a phosphine-oxide (**L3**, complex **C**, right) without changing the basic structure of catalyst-substrate complex.

the phosphine oxide takes the role of the urea group: forming a hydrogen bond with the OH group of the substrate. Additionally, we could further optimize the strength of the hydrogen bond by changing the substituents on the phosphine oxide group for methyl groups. NMR studies on a solution of complex  $\text{Rh}(\text{L3})(\text{L5})(\text{cod})\text{BF}_4$  and  $\text{Rh}(\text{L4})(\text{L5})(\text{cod})\text{BF}_4$  showed that indeed complexes are formed that are very similar to that of  $\text{Rh}(\text{L1})(\text{L5})(\text{cod})\text{BF}_4$ . In line with a stronger binding between the ligands, a large shift of the NH in  $^1\text{H}$  NMR was observed with the bis-phosphine monoxide ligands (BPMP). Importantly, 2D COSY NMR experiments showed that the hydrogen bonds between the catalyst and the substrate in complex  $[\text{Rh}(\text{L3})(\text{L5})(\text{S3})]\text{BF}_4$  are similar to those found for the analogues urea-based system.

To confirm that the stronger hydrogen bond also translates in better catalysis, we computed the reaction pathway of the hydrogenation of substrate **S3** by complex  $\text{Rh}(\text{L3})(\text{L5})\text{BF}_4$  using DFT methods. As for the first generation catalyst, the energy profile of the reaction displays an uphill profile and the rate-determining step is also represented by the hydride migration transition state structure **D**. The calculated pathways of the hydrogenation of substrate **S3** by complex  $[\text{Rh}(\text{L1})(\text{L5})]\text{BF}_4$  and  $[\text{Rh}(\text{L3})(\text{L5})]\text{BF}_4$  are plotted on the same graph in Figure 3 and it is clear that the predicted

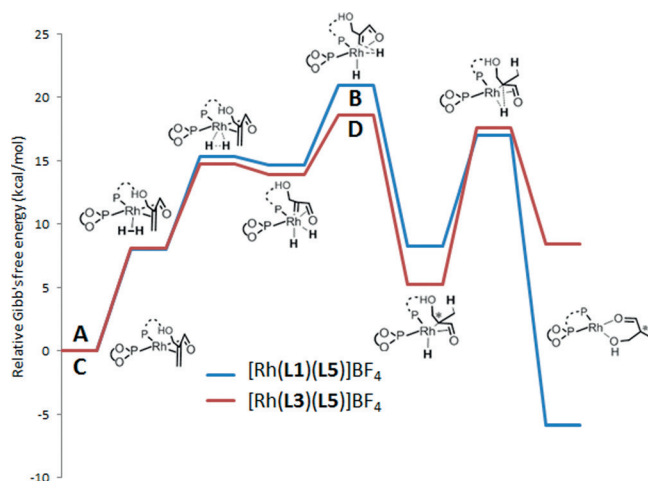


**Figure 3.** Normalized energy profiles of the unsaturated pathways for the urea-based supramolecular catalyst  $\text{Rh}(\text{L1})(\text{L5})$  (blue path) and the phosphine oxide-based supramolecular catalyst  $\text{Rh}(\text{L3})(\text{L5})$  (red path).

overall energy barrier is lower by  $2.34 \text{ kcal mol}^{-1}$  for  $[\text{Rh}(\text{L3})(\text{L5})]\text{BF}_4$ . Therefore, the stronger hydrogen bond acceptor, by going from the urea to the phosphine oxide group, is predicted to provide faster catalysis.

To verify our prediction, the performance of various rhodium complexes based on self-assembled ligands, using hydrogen bond donor **L5** and one of the hydrogen bond acceptors from **L1**–**L4**, was evaluated in the asymmetric hydrogenation of substrate **S3** by monitoring the reaction rate by gas uptake experiments (Table 2). In line with the prediction from the computational studies, the reaction is much faster when the phosphine oxide-based catalyst  $[\text{Rh}(\text{L3})(\text{L5})]\text{BF}_4$  is applied, compared to the parent  $[\text{Rh}(\text{L1})(\text{L5})]\text{BF}_4$  and also the selectivity significantly improved

**Table 2:** Hydrogenation of substrate **S3** by complexes  $[\text{Rh}(\text{L1})(\text{L5})]$ ,  $[\text{Rh}(\text{L2})(\text{L5})]$ ,  $[\text{Rh}(\text{L3})(\text{L5})]$  and  $[\text{Rh}(\text{L4})(\text{L5})]$ .<sup>[a]</sup>

| Entry | Complex  | Conv. [%] <sup>[b]</sup> | TOF <sup>[c]</sup> | ee <sup>[d]</sup> [%] |
|-------|--|--------------------------|--------------------|-----------------------|
| 1     | $\text{Rh}(\text{L1})(\text{L5})(\text{cod})\text{BF}_4$ | 98                       | 875                | 96                    |
| 2     | $\text{Rh}(\text{L3})(\text{L5})(\text{cod})\text{BF}_4$ | 100                      | 3644               | > 99                  |
| 3     | $\text{Rh}(\text{L2})(\text{L5})(\text{cod})\text{BF}_4$ | 39                       | 335                | 96                    |
| 4     | $\text{Rh}(\text{L4})(\text{L5})(\text{cod})\text{BF}_4$ | 99                       | 4561               | > 99                  |

[a] Reagents and conditions:  $[\text{Rh}] = 0.2 \text{ mM}$ , S/C ratio = 1000,  $25^\circ\text{C}$ , 20 hours,  $\text{pH}_2 = 10 \text{ bar}$ . [b] Determined by  $^1\text{H}$  NMR spectroscopy.

[c] Turnover frequencies calculated at 15% conversion. [d] Determined by HPLC.

(entry 1 vs. 2). Using **L5** in combination with **L2** results in lower activity, as in this complex the geometry is not suited to form the optimal hydrogen bond. In contrast, when  $[\text{Rh}(\text{L4})\text{-(L5)}]\text{BF}_4$  is applied the activity is even higher, as in this case the geometry of the hydrogen bond is the same, but the dimethyl phosphine oxide is a stronger hydrogen bond acceptor as the methyl groups are more electron donating than the phenyl groups. Interestingly, experiments performed at 45 °C resulted in a drop in selectivity for  $[\text{Rh}(\text{L1})(\text{L5})]\text{BF}_4$  to 93% *ee*, while the phosphine oxide-based catalyst  $[\text{Rh}(\text{L3})(\text{L5})]\text{BF}_4$  still produced the product in 96% *ee*.

In conclusion, whereas previously it has been demonstrated that the inclusion of hydrogen bonding in catalyst development can lead to unprecedented selectivity in catalysis by appropriate substrate organization at the metal complex,<sup>[5,8]</sup> we now show for the first time the successful *in silico* optimization of such catalyst. The rational approach relies on mechanistic understanding of the role of the hydrogen bonds, and subsequent *in silico* optimization of this specific interaction. In the current example, new supramolecular bidentate ligands were used, in which the urea functional group was replaced by the stronger hydrogen bond acceptor phosphine oxide in one of the building blocks. According to DFT calculations and experiments two hydrogen bonding interactions between the catalyst and the substrate exist. Increasing the strength of this hydrogen bond interaction results in a reaction pathway with a lower overall energy barrier, which as a consequence results in higher reaction rates found experimentally. In addition, the product is also produced in higher selectivity (>99% *ee*) with the rationally optimized catalyst. The development of catalysts by rational approaches is based on long-standing established parameters such as steric effects, electronic effects and bite angle effects.<sup>[10]</sup> The flourishing number of supramolecular strategies implies that non-covalent interactions should also be taken into account in the design of a catalyst. This work highlights the potential of catalyst fine-tuning by means of modification of the supramolecular interactions that can be used as a new tool to improve catalyst performance.

## Acknowledgements

This work was financially supported by a TOP grant to J.N.H.R., provided by the Dutch national science foundation (NWO). We thank Vivek Sinha for his help on the DFT calculations.

## Conflict of interest

The authors declare no conflict of interest.

**Keywords:** asymmetric hydrogenation · catalyst prediction · computational chemistry · ligand design · rhodium · supramolecular ligands

**How to cite:** *Angew. Chem. Int. Ed.* **2017**, *56*, 13056–13060  
*Angew. Chem.* **2017**, *129*, 13236–13240

- [1] a) N. B. Johnson, I. C. Lennon, P. H. Moran, J. A. Ramsden, *Acc. Chem. Res.* **2007**, *40*, 1291–1299; b) H. Shimizu, I. Nagasaki, K. Matsumura, N. Sayo, T. Saito, *Acc. Chem. Res.* **2007**, *40*, 1385–1393; c) L. A. Saudan, *Acc. Chem. Res.* **2007**, *40*, 1309–1319; d) D. J. Ager, A. H. M. de Vries, J. G. de Vries, *Chem. Soc. Rev.* **2012**, *41*, 3340–3380; e) P. Etayo, A. Vidal-Ferran, *Chem. Soc. Rev.* **2013**, *42*, 728; f) *Transition Metals for Organic Synthesis* (Eds.: M. Beller, C. Bolm), Wiley-VCH, Weinheim, **2004**.
- [2] a) B. Cornils, W. A. Herrmann, *J. of Catal.* **2003**, *216*, 23–31; b) W. A. Herrmann, *Angew. Chem. Int. Ed.* **2002**, *41*, 1290–1309; *Angew. Chem.* **2002**, *114*, 1342–1363; c) J. Meeuwissen, J. N. H. Reek, *Nat. Chem.* **2010**, *2*, 615–621; d) G. L. Hamilton, E. J. Kang, M. Mba, F. D. Toste, *Science* **2007**, *317*, 496–499; e) P. W. N. M. van Leeuwen, *Homogeneous Catalysis: Understanding the Art*, Kluwer Academic Publishers, Dordrecht, **2004**; f) J. F. Hartwig, *Organotransition Metal Chemistry: From Bonding to Catalysis*, University Science Books, Sausalito, **2009**; g) T. P. Yoon, *Science* **2003**, *299*, 1691–1693.
- [3] For reviews on high-throughput screening, see: a) W. Tang, X. Zhang, *Chem. Rev.* **2003**, *103*, 3029; b) C. Jäkel, R. Paciello, *Chem. Rev.* **2006**, *106*, 2912–2942; c) C. Gennari, U. Piarulli, *Chem. Rev.* **2003**, *103*, 3071–3100; For the use of mixture of monodentate ligands, see: d) M. T. Reetz, T. Sell, A. Meiswinkel, G. Mehler, *Angew. Chem. Int. Ed.* **2003**, *42*, 790; *Angew. Chem.* **2003**, *115*, 814; e) D. Peña, A. J. Minnaard, J. A. F. Boogers, A. H. M. de Vries, J. G. de Vries, B. L. Feringa, *Org. Biomol. Chem.* **2003**, *1*, 1087–1089; f) M. T. Reetz, O. Bondarev, *Angew. Chem. Int. Ed.* **2007**, *46*, 4523–4526; *Angew. Chem.* **2007**, *119*, 4607–4610; g) A. J. Minnaard, B. L. Feringa, L. Lefort, J. G. de Vries, *Acc. Chem. Res.* **2007**, *40*, 1267–1277.
- [4] For reviews, see: a) M. J. Wilkinson, P. W. N. M. van Leeuwen, J. N. H. Reek, *Org. Biomol. Chem.* **2005**, *3*, 2371–2383; b) B. Breit, *Angew. Chem. Int. Ed.* **2005**, *44*, 6816–6825; *Angew. Chem.* **2005**, *117*, 6976–6986; c) A. J. Sandee, J. N. H. Reek, *Dalton Trans.* **2006**, 3385–3391; d) R. Bellini, J. I. van der Vlugt, J. N. H. Reek, *Isr. J. Chem.* **2012**, *52*, 613–629; e) S. Carboni, C. Gennari, L. Pignataro, U. Piarulli, *Dalton Trans.* **2011**, *40*, 4355–4373; f) P. E. Goudriaan, P. W. N. M. van Leeuwen, M.-N. Birkholz, J. N. H. Reek, *Eur. J. Inorg. Chem.* **2008**, 2939–2958; g) M. Raynal, P. Ballester, A. Vidal-Ferran, P. W. N. M. van Leeuwen, *Chem. Soc. Rev.* **2014**, *43*, 1660–1733; For some supramolecular ligands in asymmetric hydrogenation see: h) L. Pignataro, S. Carboni, M. Civera, R. Colombo, U. Piarulli, C. Gennari, *Angew. Chem. Int. Ed.* **2010**, *49*, 6633–6637; *Angew. Chem.* **2010**, *122*, 6783–6787; i) L. Pignataro, M. Boghi, M. Civera, S. Carboni, U. Piarulli, C. Gennari, *Chem. Eur. J.* **2012**, *18*, 1383–1400; j) X.-B. Jiang, L. Lefort, P. E. Goudriaan, A. H. M. de Vries, P. W. N. M. van Leeuwen, J. G. de Vries, J. N. H. Reek, *Angew. Chem. Int. Ed.* **2006**, *45*, 1223–1227; *Angew. Chem.* **2006**, *118*, 1245–1249; k) M. N. Birkholz, N. V. Dubrovina, H. Jiao, D. Michalik, J. Holz, R. Paciello, B. Breit, A. Borner, *Chem. Eur. J.* **2007**, *13*, 5896–5907; l) F. A. J. Sandee, A. M. van der Burg, J. N. H. Reek, *Chem. Commun.* **2007**, 864–866; m) J. Meeuwissen, M. Kuil, A. M. van der Burg, A. J. Sandee, J. N. H. Reek, *Chem. Eur. J.* **2009**, *15*, 10272–10279; n) C. Chen, Z. Zhang, S. Jin, X. Fan, M. Geng, Y. Zhou, S. Wen, X. Wang, L. W. Cheng, X.-Q. Dong, X. Zhang, *Angew. Chem. Int. Ed.* **2017**, *56*, 6808–6812; *Angew. Chem.* **2017**, *129*, 6912–6916.
- [5] For reviews see: a) P. Dydio, J. N. H. Reek, *Chem. Sci.* **2014**, *5*, 2135–2145; b) H. J. Davis, R. J. Phipps, *Chem. Sci.* **2017**, *8*, 864–877; For some examples see c) T. Šmejkal, D. Gribkov, J. Geier, M. Keller, B. Breit, *Chem. Eur. J.* **2010**, *16*, 2470–2478; d) P. Dydio, C. Rubay, T. Gadzikwa, M. Lutz, J. N. H. Reek, *J. Am. Chem. Soc.* **2011**, *133*, 17176–17179; e) P. Dydio, W. Dzik, M. Lutz, B. de Bruin, J. N. H. Reek, *Angew. Chem. Int. Ed.* **2011**, *50*,

- 396–400; *Angew. Chem.* **2011**, *123*, 416–420; f) W. I. Dzik, X. Xu, X. P. Zhang, J. N. H. Reek, B. de Bruin, *J. Am. Chem. Soc.* **2010**, *132*, 10891–10902; g) P. Fackler, S. M. Huber, T. Bach, *J. Am. Chem. Soc.* **2012**, *134*, 12869–12878; h) S. Das, C. D. Incarvito, R. H. Crabtree, G. W. Brudvig, *Science* **2006**, *312*, 1941–1943; i) P. Dydio, J. H. N. Reek, *Angew. Chem. Int. Ed.* **2013**, *52*, 3878–3882; *Angew. Chem.* **2013**, *125*, 3970–3974.
- [6] a) J. M. Brown, P. A. Chaloner, *J. Chem. Soc. Chem. Commun.* **1978**, 32; b) J. M. Brown, P. A. Chaloner, *Tetrahedron Lett.* **1978**, *19*, 1877; c) J. M. Brown, P. A. Chaloner, *J. Chem. Soc. Chem. Commun.* **1979**, 613; d) J. M. Brown, P. A. Chaloner, *J. Chem. Soc. Chem. Commun.* **1980**, 344; e) J. M. Brown, P. A. Chaloner, R. Glaser, S. Geresh, *Tetrahedron* **1980**, *36*, 815; f) J. Halpern, D. P. Riley, A. S. C. Chan, J. J. Pluth, *J. Am. Chem. Soc.* **1977**, *99*, 8055; g) A. S. C. Chan, J. Halpern, *J. Am. Chem. Soc.* **1980**, *102*, 838; h) A. S. C. Chan, J. J. Pluth, J. Halpern, *J. Am. Chem. Soc.* **1980**, *102*, 5952; i) J. Halpern, *Science* **1982**, *217*, 401.
- [7] a) C. Poree, F. Schoenbeck, *Acc. Chem. Res.* **2017**, *50*, 605–608; b) K. N. Houk, F. Liu, *Acc. Chem. Res.* **2017**, *50*, 539–543; For a recent contribution in this field see: Y. Guan, S. E. Wheeler, *Angew. Chem. Int. Ed.* **2017**, *56*, 9101–9105; *Angew. Chem.* **2017**, *129*, 9229–9233.
- [8] P.-A. R. Breuil, F. W. Patureau, J. N. H. Reek, *Angew. Chem. Int. Ed.* **2009**, *48*, 2162–2165; *Angew. Chem.* **2009**, *121*, 2196–2199.
- [9] I. D. Gridnev, T. Imamoto, *Chem. Commun.* **2009**, 7447–7464.
- [10] a) C. A. Tolman, *Chem. Rev.* **1977**, *77*, 313–348; b) C. P. Casey, G. T. Whiteker, *Isr. J. Chem.* **1990**, *30*, 299–304; c) P. W. N. M. van Leeuwen, P. C. J. Kamer, J. N. H. Reek, P. Dierkes, *Chem. Rev.* **2000**, *100*, 2741–2769; d) C. A. Tolman, *J. Am. Chem. Soc.* **1970**, *92*, 2953–2956.

Manuscript received: July 27, 2017

Accepted manuscript online: August 23, 2017

Version of record online: September 12, 2017